Ascent Heating Thermal Analysis on the Spacecraft Adaptor (SA) Fairings and the Interface with the Crew Launch Vehicle (CLV)

XiaoYen Wang, James Yuko, and Brian Motil
NASA Glenn Research Center
Cleveland, Ohio 44135

Abstract

When the crew exploration vehicle (CEV) is launched, the spacecraft adaptor (SA) fairings that cover the CEV service module (SM) are exposed to aero heating. Thermal analysis is performed to compute the fairing temperatures and to investigate whether the temperatures are within the material limits for nominal ascent aero heating case. Heating rates from Thermal Environment (TE) 3 aero heating analysis computed by engineers at Marshall Space Flight Center (MSFC) are used in the thermal analysis. Both MSC Patran/Pthermal and C&R Thermal Desktop/Sinda models are built to validate each other. The numerical results are also compared with those reported by Lockheed Martin (LM) and show a reasonably good agreement.

Introduction

The ascent heating on the crew exploration vehicle (CEV) is analyzed by using computational fluid dynamics (CFD) and engineering codes at MSFC. Thermal Environment 3 (TE3) heating data is used in this work. One of the major concerns is with the SA fairings covering the CEV service module (SM) and the SM/crew launch vehicle (CLV) flange interface. The TE3 heating rate is a function of time, wall temperature, and the spatial locations. Two commercial software packages, Thermal Desktop (TD) and MSC Patran, are used in this analysis.

TD/Sinda has been widely used for spacecraft-related thermal analysis including orbital heating. TD is the pre- and post-processor for Sinda, which is a finite-difference-based solver. In TD, the geometry is built and meshed, the boundary conditions are defined, and then Sinda is used to compute temperatures. Some geometry-related issues in TD are listed as follows: (i) TD can only use very simple geometries, such as cone, cylinder, disk, ellipsoid, rectangle, sphere, etc., for surfaces, and solid brick, solid cone, solid cylinder, and solid sphere for solid geometry. More complicated geometry involving curvatures cannot be modeled in a straightforward and accurate way; (ii) Most CAD geometry will not be recognized in TD. Only lines or points from geometry imported from CAD files can be used to build TD surfaces or solids; (iii) TDmesh is available and also under improvement in TD. It can create finite element mesh (FEM) for any solids/surfaces defined in AutoCAD and ACIS file. However, the boundary information is not available, which results in difficulties in defining the boundary conditions (BCs); (v) TD can read in FEM from NASTRAN, FEMAP, and other sources, but no boundary information is transferable upon import. The user has to deal with thousands or more

FEM with no geometry information, which is the fundamental data that users need for defining BCs. Because of TD's limitations on modeling the geometry, conduction becomes very difficult to model.

To define the BCs, a conductor can be defined using the node-to-node, node-to-nodes, or node-to-surface options. A contactor can be defined using the surface-to-surface or edge-to-surface options. Heat loads can be defined on nodes, surfaces or solids. Conductance, contact resistance, and heat load are all only time or temperature dependent. There is no straightforward method to define boundary conditions that are dependent on time, temperature, and spatial locations simultaneously. Extra programs need to be added within Sinda to interact with TD, which is not straightforward and errors are easily created.

MSC Pthermal is a finite element-based thermal solver. MSC Patran is the pre- and post-processor for Pthermal. It can import geometry from ProE parts or assembly files, IGES files, and step files. It does not need to convert imported CAD geometry into Patran geometry. MSC Patran can use most CAD solids or surfaces and can be used and/or meshed right away, but some geometry might need modifications or simplifications for the purpose of thermal analysis. It saves labor and can model any complicated geometry in a simple way. Regarding the BCs, the convection, contact resistance, and heat load can be functions of time and spatial locations, or functions of the wall temperature. Different ways to impose BCs in MSC Patran are available and straightforward.

The TE3 heating rate will be presented first and the simplification of the data representation is described. Then the thermal models and results obtained by using TD/Sinda, and MSC Patran/pthermal are presented. The temperature results are compared; finally, the conclusion is given.

The TE3 ascent heating rate on SA

The ALAS-11 TE3 ascent heating rates are gathered at certain body points (BPs) on CEV and CLV. On the section of the SA, there are three BPs along the axial direction, denoted as BP 016x03, 016x05, 016x09, and are shown in figure 1(a). On the SM/CLV flange interface, the BPs are denoted as 021x20, 021x21, 021x22, 021x23, and 021x24 and are shown in figure 1(b), where x = 0,1,2,…7 for eight points uniformly distributed along circumferential direction. In figure 1(c), the geometry of the SM/CLV interface is shown and each part name will be used in the following discussion.

As an example, the heating rates at all BPs on the SA are plotted in figure 2 for the cold wall case. The heating rate on the SA is nearly uniform along the axial and circumferential directions. To simplify the thermal analysis, the heating rate at BP 016703 (x=802 in., $\theta = 315°$) has the highest heating rate for most of the time, and will be used over the entire surface of the outer face sheet (OFS) of the SA fairings. For the BPs on the SM/CLV interface, the detailed heating rate is referred to (ref. 1) and will not be plotted here. The heating rate at $\theta = 0$ is used for all different axial locations.

(a) BPs on SA

016x01
016x00   016x03
015x03   016x05   016x09

Fairing BP from Previous Slide

Internal Configuration of CEV flange TBD

021x20
021x21   021x22
021x24
021x23

(b) SM/CLV interface BPs

(c) SM/CLV interface part names

Fairing

Linear shaped charge (LSC)

SM ring

Back cone

SM flange

CLV flange
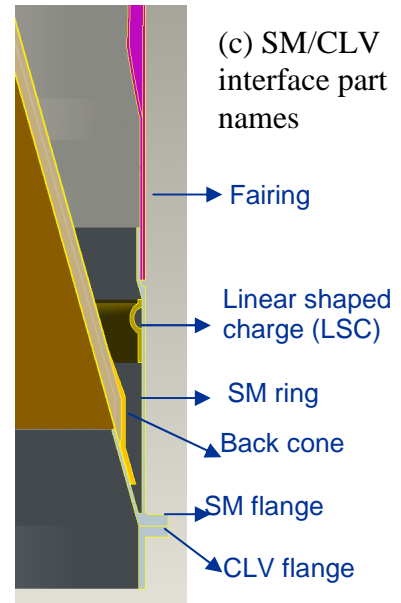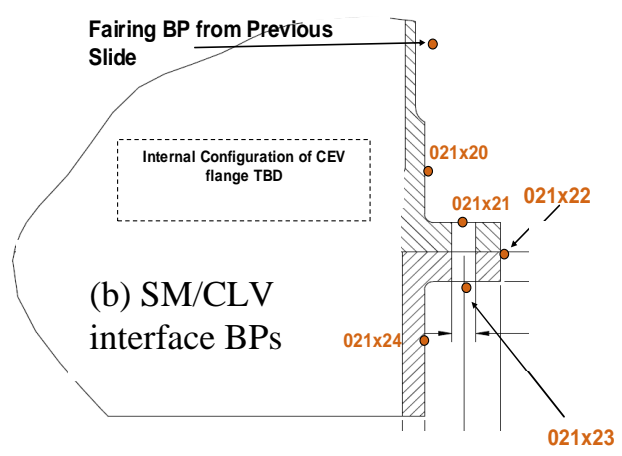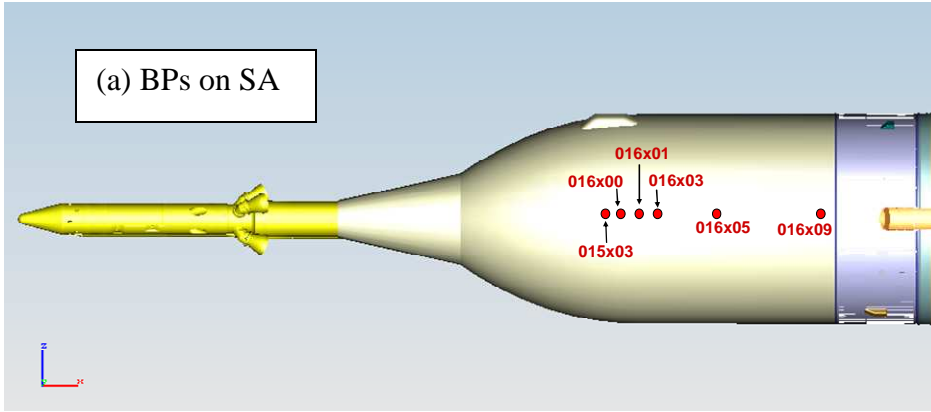
Figure 1.—The TE3 BPs on SA and SM/CLV interface flange, and the name of each part on SM/CLV interface.

BP 016x03

BP 016x05
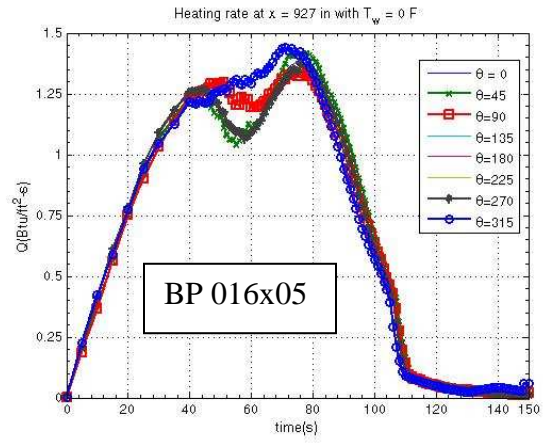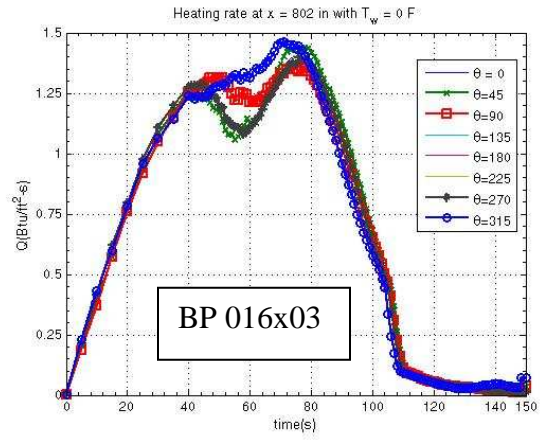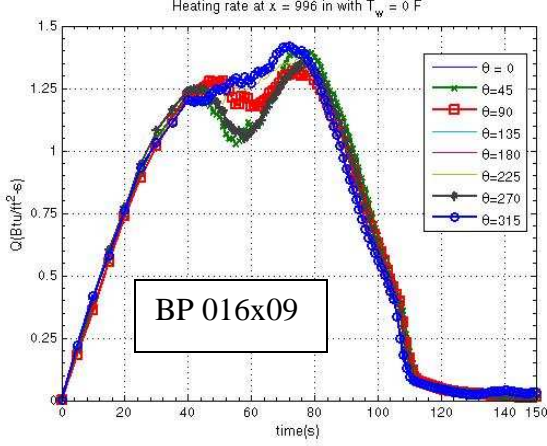
Figure 2.—TE3 heating rate at the body points on the SA for the cold wall case.

The heating rates provided in TE3 data include gas convection, gas radiation, particle convection, and particle kinetic energy heat transfer. For the ascent heating on the SA, only the gas convection contributes to the heating rate. Therefore, the total heating rate can be defined as

$$\dot{q}_{total} = h_c (H_{rec} - H_{wall}) \qquad (1)$$

where h_c is the enthalpy-based heat transfer coefficient, H_{rec} is the gas recovery enthalpy, H_{wall} is the gaseous wall enthalpy and defined as

$$H_{wall} = 0.2345 T_{wall} + 9.786 x 10^{-6} T_{wall}^2 + 943.6 / T_{wall} - 1.57 \qquad (2)$$

with T_{wall} being the wall temperature in Rankine. The given time history of h_c changes slightly when the wall temperature changes from 0 to 2000 °F. It is obvious that $\dot{q}_{total}$ is not a linear function of T_{wall}. With the given ascent heating data, $\dot{q}_{total}$ is plotted as the function of T_{wall} in figure 3. It can be seen that $\dot{q}_{total}$ is almost a linear function of T_{wall} when T_{wall} < 760 °F. Since the material temperature limit on the SA is far below 760 °F, it can be assumed that

$$H_{wall} = 0.2345 T_{wall} \qquad (3)$$

Based on this assumption, the enthalpy-based heat transfer coefficient (h_c) can be easily converted into the temperature-based heat transfer coefficient (h_t) as follows:

$$h_t = c_p h_c, \quad T_{rec} = H_{rec} / c_p, \quad T_{wall} = H_{wall} / c_p \qquad (4)$$

where c_p = 0.2345 Btu/lbm-°F for air, and T_{rec} is the air recovery temperature. The so-obtained h_t and T_{rec} are plotted in figure 4. It shows that h_t changes when the wall temperature is different. The heat rates computed based on h_t and h_c are plotted in figure 5, which shows that h_t gives slightly higher heat flux than h_c. The convection BC on the fairing surface is only time dependent when using h_t. Thermal analysis presented here is on the conservative side. It is the worst case for the temperatures on the SA fairings.
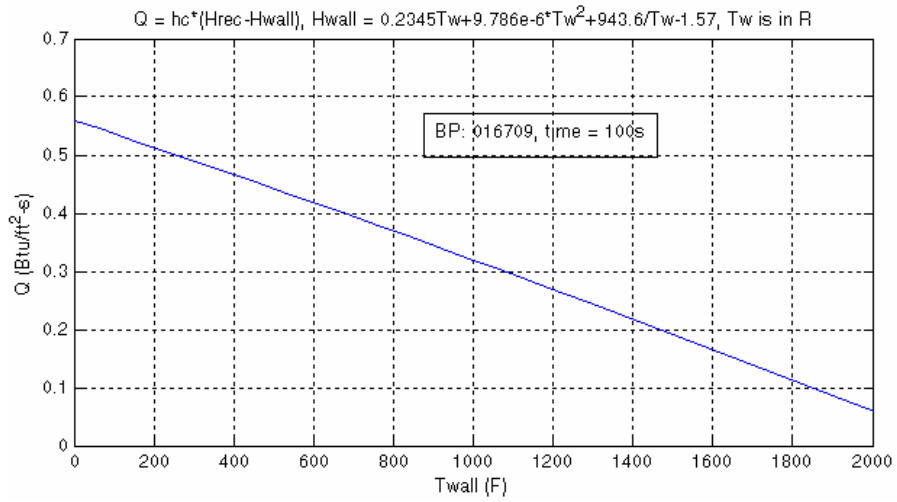
Figure 3.—The heating rate versus the wall temperature at BP 016709 at t =100 s.
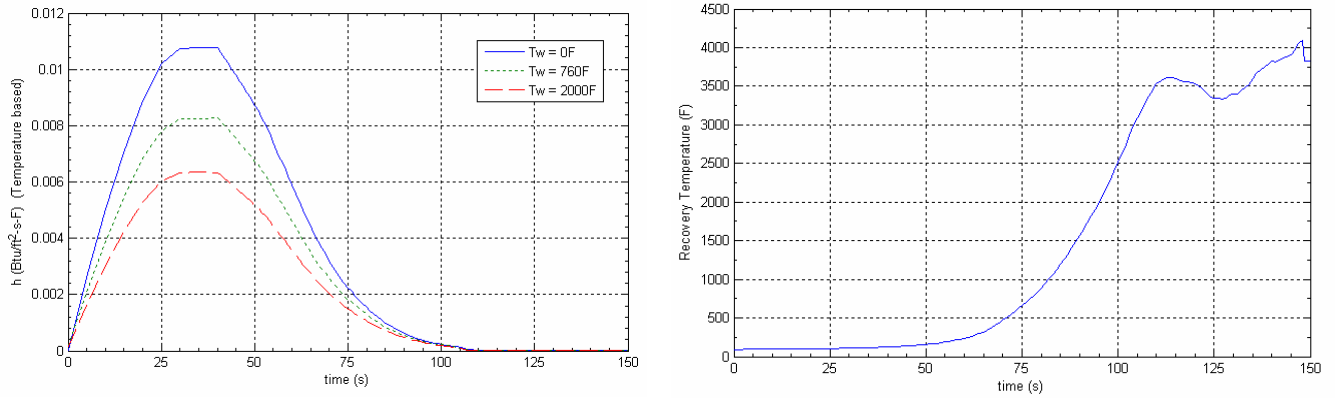
Figure 4.—The computed temperature-based h and air recovery temperature.
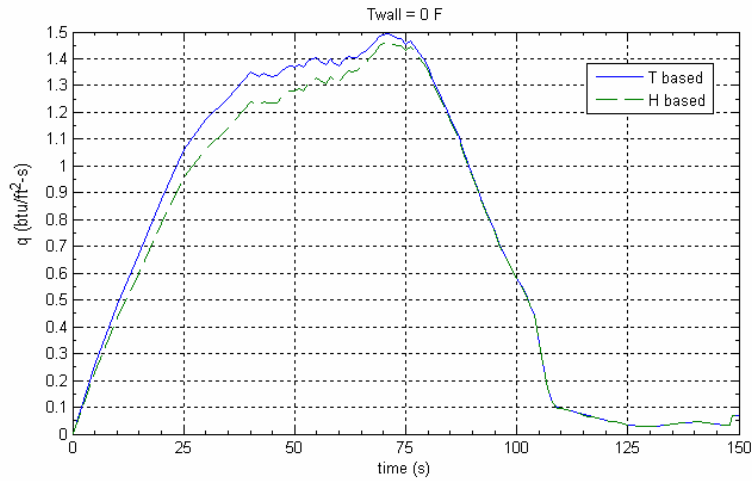
Figure 5.—The comparison of the enthalpy-based and temperature-based heating rate.

Thermal Model in Thermal Desktop

In the TD model, the ACIS file is imported to build TD surfaces and solids. The SA fairings are formed by an OFS, a Honeycomb (H/C) core, and an inner face sheet (IFS). Each has three pieces along the circumferential direction. The OFS and IFS are 0.0424-in.- thick composite, and H/C core is 1.5-in.-thick aluminum. Each piece is modeled as a cylindrical surface with a defined thickness.

The convection BCs are defined using the node-to-surface option. The air recovery temperature is defined at the node, and h_t is defined on the OFS of SA fairing and SM/CLV interface. The contact resistance between the inner surface of the OFS to H/C core, and the outer surface of the IFS to H/C core is $h = 0.694$ Btu/hr-in^2-°F for low resistance. The IFS to SM ring (edge to surface) is $h = 0.0014$ Btu/hr-in-°F, assuming that a minimum heat transfers to the ring from IFS and the overlap between IFS and ring is 2.0 in. The SM ring to back cone (edge to surface) is $h = 14$ Btu/hr-in-°F for low resistance. The flange to ring on CLV, flange to ring on SM, and CLV flange to SM flange (surface to surface) is $h = 6.94$ Btu/hr-in^2-°F for low resistance. The outer surface of the SA fairing radiates to the ambient air at $T = 50$ °F, and the inner surface of the fairing radiates to the radiator at $T = 70$ °F.

The SA fairings jettison at $t = 150$ s. The temperature contour at $t = 100.8$ s is plotted in figure 8 for the OFS, H/C core, and IFS, when the fairings reach the maximum temperature. Figure 9 shows the corresponding contour for the SM/CLV flange interface at $t = 172.8$ s. The time history of the temperature on OFS, H/C core, IFS, and SM/CLV interface is plotted in figure 10, showing that the temperature could reach 275 °F on the OFS and 225 °F on the SM ring. Note that no heat load is defined on the hinge (fig. 9). Since the hinge is a protuberance above the SM ring, the local area next to the hinge could have a higher heating rate.
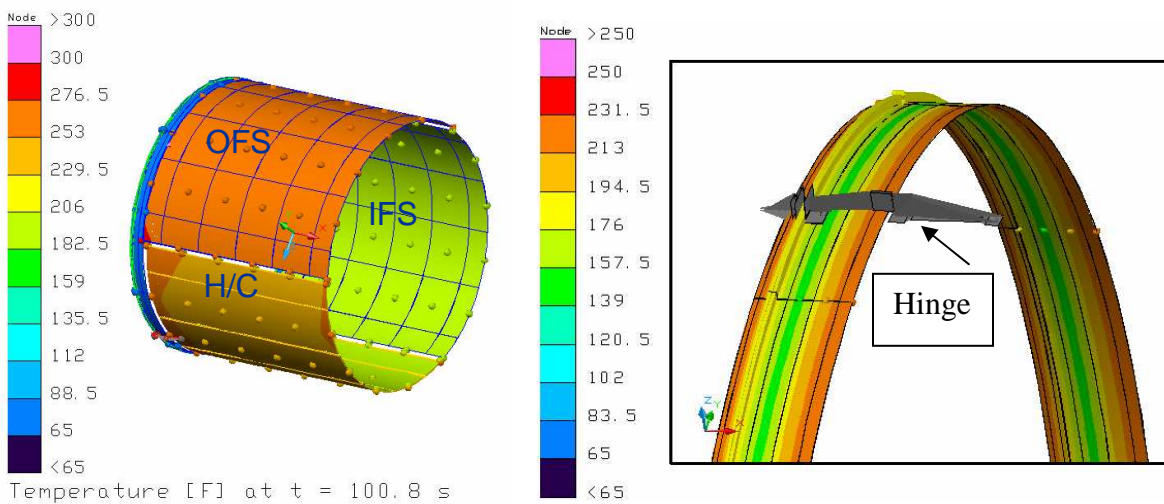
Figure 8.—TD results of OFS, H/C core, and IFS.

Figure 9.—TD result of SM ring and SM/ CLV flange interface at $t = 172.8$ s.
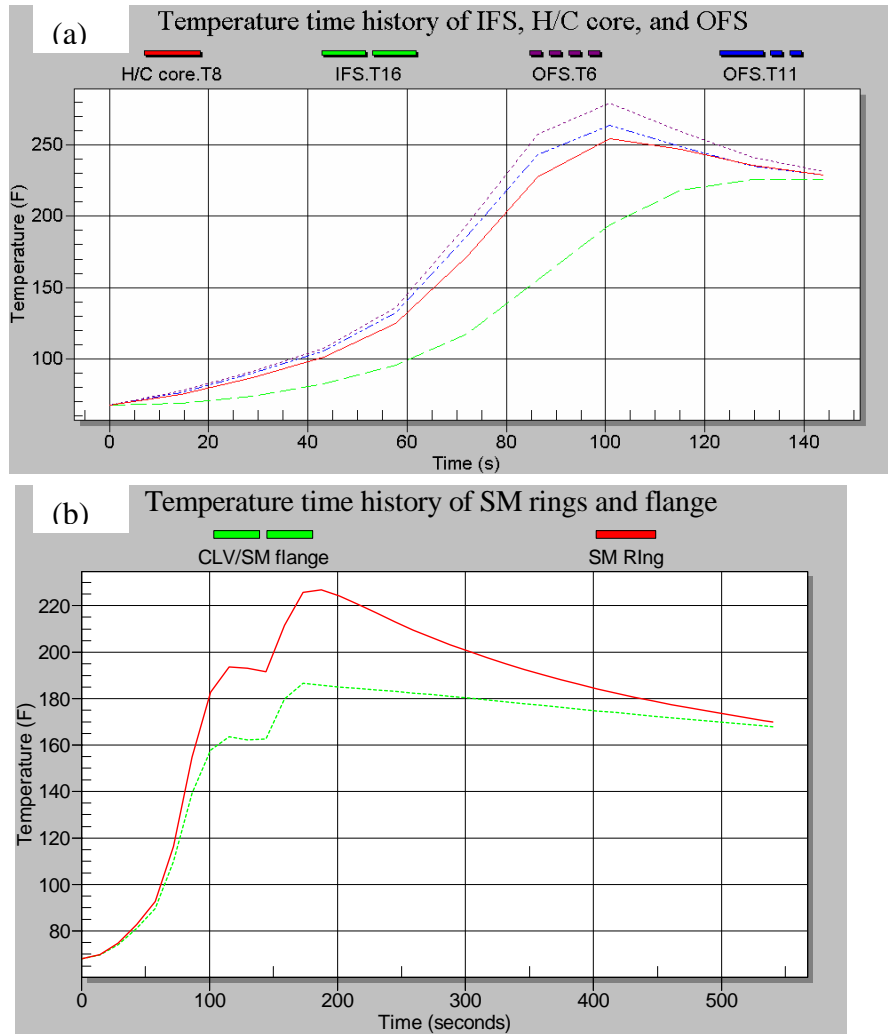
Figure 10.—Time history of the temperature on OFS, H/C, IFS, SM ring, and SM/CLV flange interface (TD results).

Thermal Model in MSC Patran/Pthermal

In the MSC Patran model, there are 116,552 nodes and 290,249 elements. The BCs are the same as those used in the TD model. The Pthermal temperature contour on the SA fairings, IFS, H/C core, and OFS at $t = 100$ s are plotted in figure 11. The MSC Patran model has more accurate modeling of the actual geometry of OFS, H/C core, and IFS. It shows more temperature variations across each part since it has different thicknesses even with the same ascent heating rates are applied. The temperature time history on the OFS, H/C core, and IFS are plotted in figure 12. It shows that the maximum temperature on the

fairings reaches 300 °F at t = 100 s. The corresponding results for the SM/CLV interface structures are plotted in figures 13 and 14, showing that the maximum temperature there reaches 230 °F at t = 170 s.
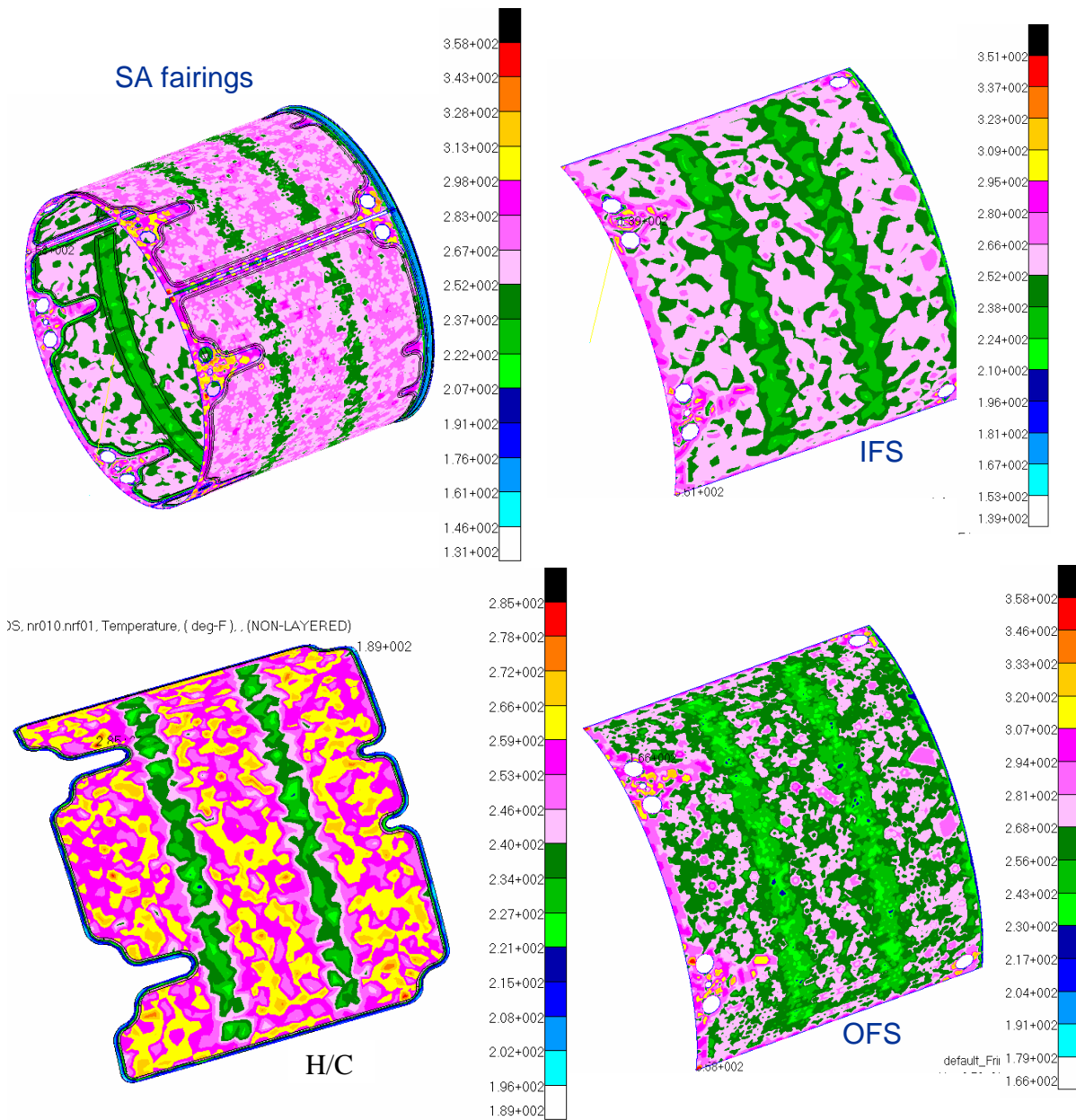
Figure 11.—MSC Patran result of OFS, H/C, and IFS at t =100 s.
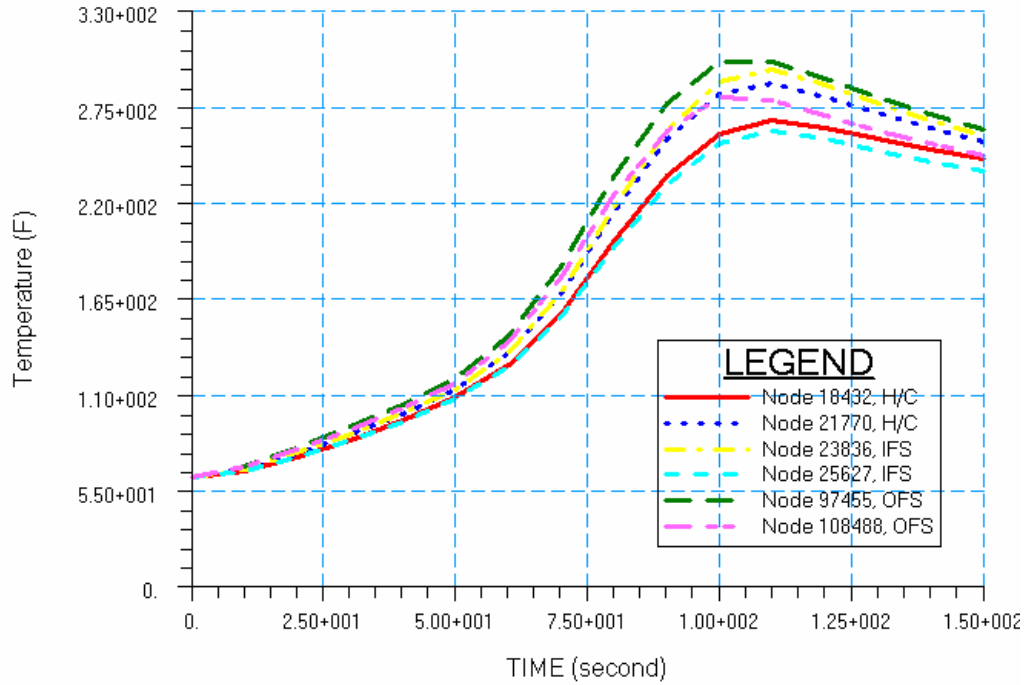
Figure 12.—Time history of the temperature on OFS, IFS, and H/C (MSC Patran results).
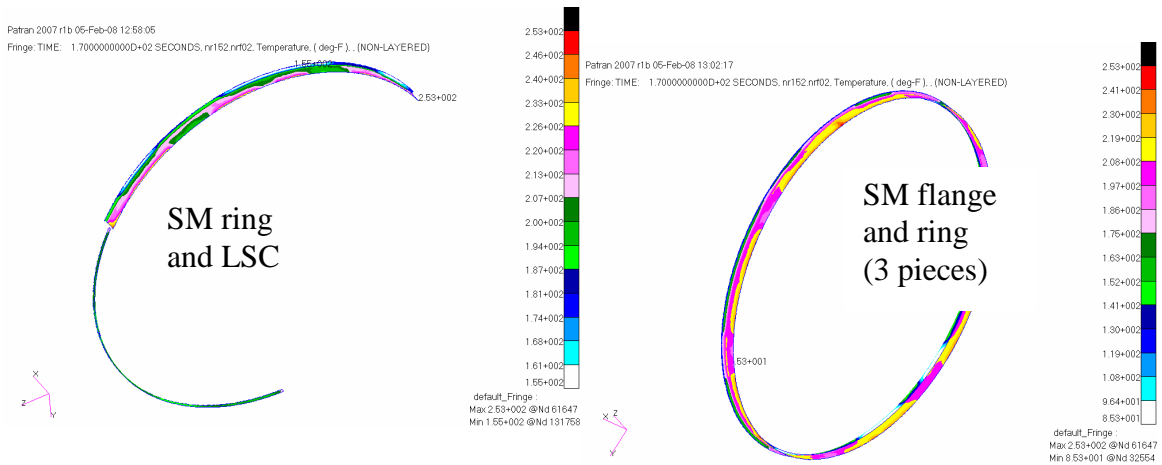
Figure 13.—MSC Patran result of SM ring and SM/CLV flange interface.
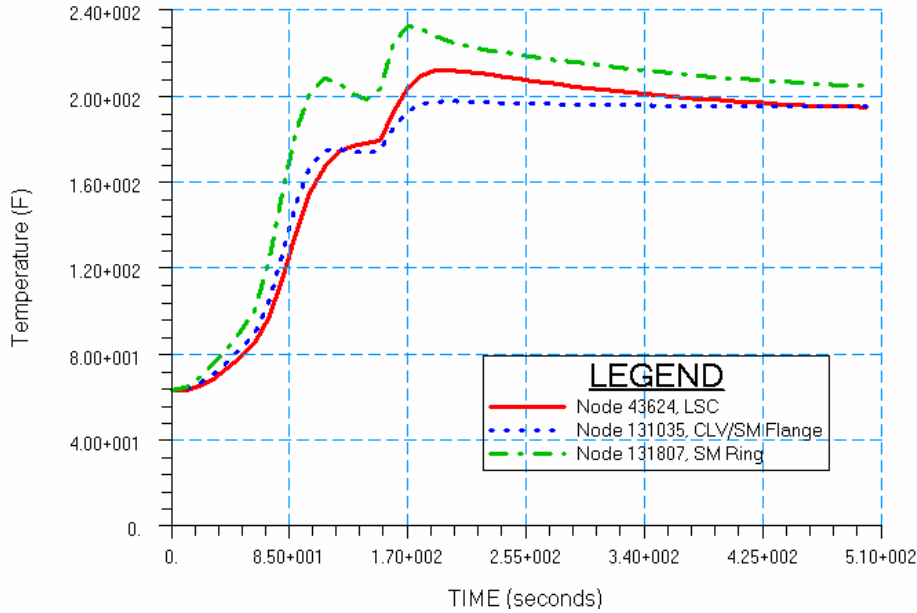
Figure 14.—MSC Patran result of SM ring and SM/CLV flange interface.

The detailed temperature comparison between the TD results, MSC Patran results, and LM reported results (ref. 2) are shown in table I, showing a reasonable agreement. The maximum allowable temperature is also listed. For the SA fairings, the temperature is within the limit. However, the temperatures on SM/CLV flanges and SM ring are close to or above the temperature limit. Although the analysis presented here used a conservative heating rate, the hinge effect is not included. The hinge is a large protuberance on the SA fairing and will results higher heat transfer. Necessary thermal protections will be considered at the local area on the SM/CLV flanges and SM ring close to the hinge. Further analysis on the thermal protection is necessary.

Conclusions

The ascent heating thermal analysis on SA fairings and SM/CLV flange interface are performed using MSC Patran and C&R TD. Both TD and MSC Patran results agree reasonably well with those reported by LM on fairings and SM/CLV flange interface. Both results predict higher temperature than LM reported because of the use of temperature-based heat transfer coefficient in the analysis, which gives higher heat flux. The SA fairing reaches maximum temperature (280 °F) at $t = 100$ s. The hottest spots are next to hinges, and the areas that are not covered by honeycomb (as shown in MSC Patran model, 320 °F). The SM flange and ring and LSC reach maximum temperature at $t = 170$ s. The temperature at the corner of the ring could reach 253 °F. With the hinge effects, the fairing temperature under the hinges could get higher than predicted here. Necessary thermal protection is needed for the areas on the SM/CLV flanges and SM ring that are next to the hinge.

Acknowledgments

TABLE I.—COMPARISON OF MAXIMUM TEMPERATURE ON SA FAIRING
AND SM/CLV FLANGE INTERFACE

	Max temperature[a], °F			Max allowed temperature, °F
	LM result	Current TD result	Current MSC Patran result	
Fairing (OFS)	272	280	280	325 to 400
CLV/SM flange	184	186	196	150 to 180
SM ring	200	225	232	220
LSC	200	NA	210	220

[a]No hinge localized heating (with margin of 1.35 included in TE3 data)

1. M. D'Agostino, CxP 72068, "ARES-I design analysis cycle-2 TE3 thermal environments data book," Oct. 30, 2007.
2. R. Barsoum, private communications, Lockheed Martin, Houston, TX.